

Chemical evolution model to derive metallicity distributions for each stellar population

Hidetomo Homma

National Astronomical Observatory of Japan, 2-21-1 Osawa, Mitaka, Tokyo 181-8588, JAPAN
email: hidetomo.homma@nao.ac.jp

Abstract. We have constructed a chemical evolution model in order to reproduce the both metallicity distribution functions (MDFs) of red giant branch stars (RGBs) and RR Lyrae stars (RRLs) of a dwarf galaxy, simultaneously. The detailed chemical abundances of RGBs of the Local Group dwarf galaxies have been measured by spectroscopic observations. Moreover, the metallicity of RRLs of a dwarf galaxy are estimated by using the theoretical period-luminosity relations in the previous study and it is found that the mean metallicity of RRLs are lower than that of RGBs. In order to investigate the MDFs of RGBs and RRLs, we combine our chemical evolution model with the stellar evolutionally isochrones and calculate the metallicity of RGBs and RRLs, respectively. As a result, our chemical evolution model reproduces the peak metallicity of both MDFs of RGBs and RRLs of Sculptor and Fornax dwarf spheroidal galaxies (dSphs), simultaneously. Therefore, it is found that the difference of the mean metallicity between RGBs and RRLs are caused by the effects of stellar evolution. Moreover, by using the theoretical period-luminosity-metallicity relation of the RRLs, our chemical evolution model determines that the distance modulus of Sculptor and Fornax dSphs are 19.68 ± 0.09 and $20.81^{+0.13}_{-0.11}$, respectively. However, our model underestimates the number of metal-rich RRLs ($[\text{Fe}/\text{H}] > -1.5$) of Fornax dSph. This result suggests that the mass-loss rate of metal-rich RGBs would be larger than that of metal-poor RGBs.

Keywords. galaxies: abundances, galaxies: dwarf, galaxies: evolution, galaxies: individual (Sculptor, Fornax)

1. Introduction

The dwarf galaxies in the Local Group are good laboratories to investigate detailed galaxy evolution since we can observe the individual stars. By comparing the stellar color magnitude diagram (CMD) and theoretical stellar population synthesis model, many previous studies have derived the detailed star formation history (SFH) of dwarf galaxies (e.g., [de Boer *et al.* \(2012a, b\)](#)). Moreover, the spectroscopic observations of individual red giant branch stars (RGBs) of dwarf galaxies have shown the metallicity distribution functions (MDFs) of dwarf galaxies (e.g., [Kirby *et al.* 2010](#)). Furthermore, the metallicity of RR Lyrae stars (RRLs) are estimated from the theoretical period-luminosity-metallicity (PLZ) relation. It is shown that the MDF of RRLs is narrower and more metal-poor than that of RGBs ([Martínez-Vázquez *et al.* 2016a](#)). These differences are caused by the effects of age and metallicity on the stars, that is, the metal-rich and young stars are too red to be RRLs. Therefore, such differences of MDFs between different stellar populations (i.e., RGBs and RRLs) reflect the chemical evolution of dwarf galaxies.

The theoretical chemical evolution model is a basic tool to investigate the chemical evolution of galaxies. In order to reproduce both MDFs of RGBs and RRLs of dwarf galaxies,

simultaneously, we have constructed a detailed chemical evolution model combining the stellar population synthesis model. In this study, we investigate the detailed chemical evolution of the two Local Group dwarf galaxies, Sculptor and Fornax dwarf spheroidal galaxies (dSphs) by using this chemical evolution model.

2. Chemical Evolution Model

In this work, we combine the chemical evolution model with the stellar population synthesis model to calculate the metallicity distributions of RGBs and RRLs of a galaxy and compare them with the observed data.

We adopt the chemical evolution model of [Homma *et al.* \(2015\)](#) which calculates the chemical evolution of a galaxy according to the input SFH. The equations of the chemical evolution are as follows.

$$\frac{d}{dt} (Z_i M_{\text{gas}}) = -\Psi(t)Z_i(t) + E_i(t) - \dot{M}_{\text{out}}(t)Z_i(t) + \dot{M}_{\text{in}}(t)Z_{i,\text{in}}(t) \quad (2.1)$$

$$\frac{M_{\text{gas}}(t)}{10^6 M_{\odot}} = \left(\frac{\Psi(t)}{10^6 M_{\odot} \text{Gyr}^{-1}} \right) / A_{\star} \quad (2.2)$$

$$\dot{M}_{\text{out}}(t) = A_{\text{out}} (\dot{N}_{\text{SNII}}(t) + \dot{N}_{\text{SNIa}}(t)) \quad (2.3)$$

where Z_i , E_i , M_{gas} , M_{out} , and M_{in} are the metallicity for element i , stellar ejecta for element i , gas mass, outflow gas mass, and infall gas mass, respectively. Ψ is the input SFH of a dwarf galaxy. We adopt SFHs of Sculptor and Fornax dSphs derived by [de Boer *et al.* \(2012a, b\)](#). We assume that the star formation rate is proportional to the gas mass and the outflow rate is proportional to the number of supernovae ($N_{\text{SNII, Ia}}$). A_{\star} and A_{out} are the free parameters of this model. The chemical evolution model derives the age-metallicity relation of the dwarf galaxy.

In order to derive the MDFs of each stellar population, we calculate the stellar population synthesis model by using the age-metallicity relation, SFH, and PARSEC isochrones of [Bressan *et al.* \(2012\)](#). We adopt the mass-loss on RGB as $\eta = 0.2$ that is determined by [Miglio *et al.* \(2012\)](#). From the stellar population synthesis model, we construct the MDFs of the RGBs and RRLs which satisfy the photometric criterion (i.e., luminosity and color range) of the sample.

The sample of the RGBs and RRLs are obtained from the observations of [Kirby *et al.* \(2010\)](#), [Martínez-Vázquez *et al.* \(2016a\)](#), and [Karczmarek *et al.* \(2017\)](#). While the metallicity of RGBs are spectroscopically determined by [Kirby *et al.* \(2010\)](#), those of RRLs are estimated from the inverse PLZ relation of [Marconi *et al.* \(2015\)](#) as follows.

$$[\text{Fe}/\text{H}] = \frac{m - (m - M)_0 - b \log P - a}{c} \quad (2.4)$$

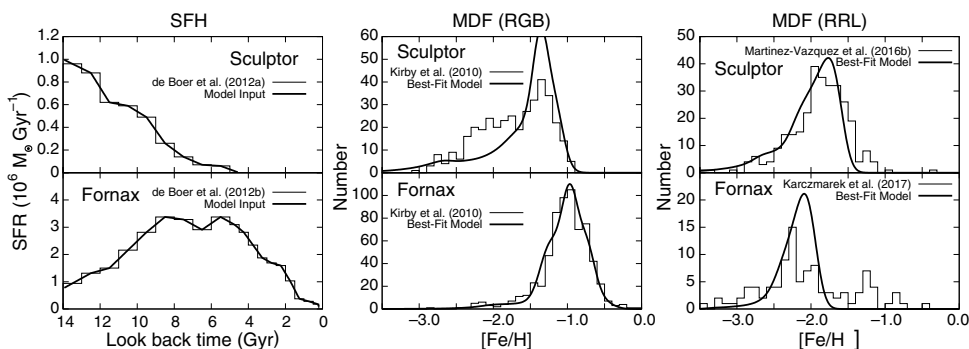
where m and P are the mean magnitude and the pulsation period of an RRL, respectively. The coefficients of a , b , and c are shown in [Marconi *et al.* \(2015\)](#). We adopt the observed properties of RRLs of Sculptor and Fornax dSphs in [Martínez-Vázquez *et al.* \(2016b\)](#) and [Karczmarek *et al.* \(2017\)](#), respectively. From these literature, we adopt the distance modulus of Sculptor and Fornax dSphs as $(m - M)_0 = 19.62$ and 20.818 , respectively. By comparing the MDFs of our model and observed data, we calculate the likelihood of the model and explore the best-fit model which maximizes the likelihood by using Markov-Chain Monte-Carlo method.

3. Results

Our models reproduce the peak metallicity of both MDFs of RGBs and RRLs, simultaneously, and reproduce the metallicity range of RGBs (see Figure 1). As shown in Table 1, the best-fit values of A_{\star} and A_{out} are similar to those of [Homma *et al.* \(2015\)](#), i.e., the

Table 1. The best-fit model parameters

dSphs	$\log A_*$	$\log[A_{\text{out}}(M_{\odot} \text{SN}^{-1})]$
Sculptor	$-1.33^{+0.25}_{-0.21}$	$3.73^{+0.07}_{-0.08}$
Fornax	$-1.01^{+0.10}_{-0.01}$	$3.15^{+0.02}_{-0.01}$

**Figure 1.** The input SFHs (left) and the best-fit MDFs of RGBs (middle) and RRLs (right) of Sculptor and Fornax dSphs.

inefficient star formation and large gas outflow of Sculptor and Fornax dSphs result in the lower metallicity than that of the Milky Way ($[\text{Fe}/\text{H}] \sim 0.0$). While our model reproduces the metal-poor RRLs, we underestimate the number of metal-rich RRLs ($[\text{Fe}/\text{H}] > -1.5$). In order to relax the discrepancy of the number of metal-rich RRLs, we discuss the effects of the value of distance modulus and the mass-loss on RGBs.

4. Discussion

The sample metallicity of RRLs depends on the value of distance modulus. As shown in the equation (2.4), the large value of the distance modulus results in the small metallicity of the RRLs. Therefore, in order to determine the best-fit value of the distance modulus of Sculptor and Fornax dSphs, we set the distance modulus as a free parameter in our model and explore the best-fit value reproducing both MDFs of RGBs and RRLs, simultaneously.

The best-fit values of distance modulus of Sculptor and Fornax dSphs are $(m - M)_0 = 19.68 \pm 0.09$ and $20.81^{+0.13}_{-0.11}$, respectively. The best-fit distance modulus of Sculptor dSph is larger than that of Martínez-Vázquez *et al.* (2016b) ($(m - M)_0 = 19.62 \pm 0.04$). The model for the best-fit distance modulus reproduce the peak and range of MDFs of both RGBs and RRLs, simultaneously. Moreover, the best-fit value of distance modulus of Sculptor dSph is consistent with the previous studies. Pietrzyński *et al.* (2008) determined the distance modulus of Sculptor dSph as $(m - M)_0 = 19.67 \pm 0.14$ from the period-luminosity relation of RRLs and Rizzi (2002) determined that as $(m - M)_0 = 19.66 \pm 0.15$ and 19.64 ± 0.08 from the analysis of the horizontal branch stars (HBs) and the tip of red giant branch stars, respectively. However, since the best-fit distance modulus of Fornax dSph is the same as that of Karczmarek *et al.* (2017), the model underestimates the number of metal-rich RRLs of Fornax dSph. Therefore, while our model reproduce both MDFs of RGBs and RRLs of Sculptor dSph and determines the best-fit distance modulus, the effect of the distance modulus on the model is not enough to relax the underestimate of the metal-rich RRLs of Fornax dSph. Such broad range of RRL metallicity of Fornax dSph may be explained by the effect of RGB mass-loss.

In this study, we adopt the stellar evolutionally isochrones with mass-loss on RGB as $\eta = 0.2$. Since the location of a HB on CMD is depend on the mass-loss on RGB phase, a RGB with large mass-loss evolves to a blue HB. Therefore, if the metal-rich RGBs lose large amount of gas envelope, they become blue enough to locate on the instability strip on the CMD and to be metal-rich RRLs. In the previous study, Salaris *et al.* (2013) have simulated the HBs of Sculptor dSph with varying the mass-loss of RGBs. Their simulation reproduced the photometric properties of the HBs and they suggested that the mass-loss of RGB is larger than $\eta = 0.2$ and the mass-loss of RGB is slowly increasing with increasing metallicity.

References

- Bressan, A., Marigo, P., Girardi, L., Salasnich, B., Dal C. C., Rubele, S., & Nanni, A. 2012, *MNRAS*, 427, 127
- de Boer, T. J. L., Tolstoy, E., Hill, V., Saha, A., Olsen, K., Starkenburg, E., Lemasle, B., Irwin, M. J., & Battaglia, G. 2012, *A&A*, 539, 103
- de Boer, T. J. L., Tolstoy, E., Hill, V., Saha, A., Olszewski, E. W., Mateo, M., Starkenburg, E., Battaglia, G., & Walker, M. G. 2012, *A&A*, 544, 73
- Homma, H., Murayama, T., Kobayashi, M. A. R., & Taniguchi, Y. 2015, *ApJ*, 799, 230
- Karczmarek, P., Pietrzyński, G., Górski, M., Gieren, W., & Bersier, D. 2017, *AJ*, 154, 263
- Kirby, E. N., Guhathakurta, P., Simon, J. D., Geha, M. C., Rockosi, C. M., Sneden, C., Cohen, J. G., Sohn, S. T., Majewski, S. R., & Siegel, M. 2010, *ApJS*, 191, 352
- Marconi, M., Coppola, G., Bono, G., Braga, V., Pietrinferni, A., Buonanno, R., Castellani, M., Musella, I., Ripepi, V., & Stellingwerf, R. F. 2015, *ApJ*, 808, 50
- Martínez-Vázquez, C. E., Monelli, M., Gallart, C., Bono, G., Bernard, E. J., Stetson, P. B., Ferraro, I., Walker, A. R., Dall’Ora, M., Fiorentino, G., & Iannicola, G. 2016, *MNRAS*, 461, L41
- Martínez-Vázquez, C. E., Stetson, P. B., Monelli, M., Bernard, E. J., Fiorentino, G., Gallart, C., Bono, G., Cassisi, S., Dall’Ora, M., Ferraro, I., Iannicola, G., & Walker, A. R. 2016, *MNRAS*, 462, 4349
- Miglio, A., Brogaard, K., Stello, D., Chaplin, W. J., D’Antona, F., Montalbán, J., Basu, S., Bressan, A., Grundahl, F., Pinsonneault, M., Serenelli, A. M., Elsworth, Y., Hekker, S., Kallinger, T., Mosser, B., Ventura, P., Bonanno, A., Noels, A., Silva A. V., Szabo, R., Li, J., McCauliff, S., Middour, C. K., & Kjeldsen, H. 2012, *MNRAS*, 419, 2077
- Pietrzyński, G., Gieren, W., Szewczyk, O., Walker, A., Rizzi, L., Bresolin, F., Kudritzki, R.-P., Nalewajko, K., Storm, J., Dall’Ora, M., & Ivanov, V. 2008, *AJ*, 135, 1993
- Rizzi, L. 2002 *PhD Thesis, Padova Univ.*
- Salaris, M., de Boer, T., Tolstoy, E., Fiorentino, G., & Cassisi, S. 2013, *A&A*, 559, 57